THE JOURNAL OF BIOLOGICAL CHEMISTRY VOL. 287, NO. 47, pp. 39349–39360, November 16, 2012
Published in the U.S.A.

δ-Tocopherol Reduces Lipid Accumulation in Niemann-Pick Type C1 and Wolman Cholesterol Storage Disorders*[S]

Received for publication, February 29, 2012, and in revised form, September 28, 2012 Published, JBC Papers in Press, October 3, 2012, DOI 10.1074/jbc.M112.357707

Miao Xu[‡§1], Ke Liu[‡1], Manju Swaroop[‡], Forbes D. Porter[¶], Rohini Sidhu[‖], Sally Finkes[‖], Daniel S. Ory[‖], Juan J. Marugan[‡], Jingbo Xiao[‡], Noel Southall[‡], William J. Pavan[**], Cristin Davidson[‡‡], Steven U. Walkley[‡‡], Alan T. Remaley[§§], Ulrich Baxa[¶¶], Wei Sun[‡], John C. McKew[‡], Christopher P. Austin[‡], and Wei Zheng[‡2]

From the [‡]National Center for Advancing Translational Sciences, National Institutes of Health, Bethesda, Maryland 20892, the [¶]Program in Developmental Endocrinology and Genetics, Eunice Kennedy Shriver NICHD, National Institutes of Health, Bethesda, Maryland 20892, the [‖]Diabetic Cardiovascular Disease Center, Washington University School of Medicine, St. Louis, Missouri 63110, the [**]Genetic Disease Research Branch, National Human Genome Research Institute, National Institutes of Health, Bethesda, Maryland 20892, the [‡‡]Sidney Weisner Laboratory of Genetic Neurological Disease, Rose F. Kennedy Center, Albert Einstein College of Medicine, Bronx, New York 10461, the [§§]Laboratory of Lipoprotein Metabolism, NHLBI, National Institutes of Health, Bethesda, Maryland 20892, the [§]Sir Run Run Shaw Hospital, Zhejiang University School of Medicine, Hangzhou 310016, China, and the [¶¶]Electron Microscopy Laboratory, NCI, National Institutes of Health, Bethesda, Maryland 20892

Background: Niemann-Pick disease type C and Wolman diseases are caused by mutations in genes responsible for intracellular cholesterol processing and trafficking.
Results: δ-Tocopherol reduces lysosomal accumulation of cholesterol and other lipids potentially through enhancement of lysosomal exocytosis.
Conclusion: δ-Tocopherol is a novel lead compound for drug development to treat lysosomal storage diseases.
Significance: Lysosomal exocytosis may represent a new drug target broadly applicable to lysosomal storage diseases.

Niemann-Pick disease type C (NPC) and Wolman disease are two members of a family of storage disorders caused by mutations of genes encoding lysosomal proteins. Deficiency in function of either the NPC1 or NPC2 protein in NPC disease or lysosomal acid lipase in Wolman disease results in defective cellular cholesterol trafficking. Lysosomal accumulation of cholesterol and enlarged lysosomes are shared phenotypic characteristics of both NPC and Wolman cells. Utilizing a phenotypic screen of an approved drug collection, we found that δ-tocopherol effectively reduced lysosomal cholesterol accumulation, decreased lysosomal volume, increased cholesterol efflux, and alleviated pathological phenotypes in both NPC1 and Wolman fibroblasts. Reduction of these abnormalities may be mediated by a δ-tocopherol-induced intracellular Ca^{2+} response and subsequent enhancement of lysosomal exocytosis. Consistent with a general mechanism for reduction of lysosomal lipid accumulation, we also found that δ-tocopherol reduces pathological phenotypes in patient fibroblasts from other lysosomal storage diseases, including NPC2, Batten (ceroid lipofuscinosis, neuronal 2, CLN2), Fabry, Farber, Niemann-Pick disease type A, Sanfilippo type B (mucopolysaccharidosis type IIIB, MPSIIIB), and Tay-Sachs. Our data suggest that regulated exocytosis may represent a potential therapeutic target for reduction of lysosomal storage in this class of diseases.

Niemann-Pick disease type C (NPC)[3] is caused by mutations in either the *NPC1* or *NPC2* gene, encoding two distinct lysosomal cholesterol-binding proteins (1, 2). The NPC cellular phenotype is characterized by lysosomal accumulation of unesterified cholesterol and other lipids, resulting from impaired cholesterol export from the late endosomal and lysosomal compartments (2, 3). Wolman disease is caused by mutations in the gene encoding lysosomal acid lipase (*LAL*). Deficiency of LAL function results in two distinct disease phenotypes that accumulate both cholesteryl ester and triglycerides. The early onset form is known as Wolman disease, and the late onset form is known as cholesteryl ester storage disease (3, 4). Enlarged lysosomes are a common cellular phenotype for both NPC and Wolman diseases.

Cholesterol is an essential component of cellular membranes and is central to maintaining both membrane integrity and fluidity as well as regulating membrane protein function, cell signaling, and ion permeability (5). In addition, cholesterol is the precursor molecule for synthesis of cellular components such as bile acids, oxysterols, and steroid hormones. Cholesterol homeostasis is tightly regulated at both the cellular and whole-

* This work was supported, in whole or in part, by the National Institutes of Health Intramural Research Program of the National Center for Advancing Translational Sciences, by the Intramural Research Program of the National Human Genome Research Institute, by the Intramural Research Program of the Eunice Kennedy Shriver NICHD, and by NCI, National Institutes of Health, Contract HHSN26120080001E. This work was also supported by a grant from the Ara Parseghian Medical Research Foundation.
[S] This article contains supplemental Table S1 and Figs. S1–S7.
[1] Both authors contributed equally to this work.
[2] To whom correspondence should be addressed: National Center for Advancing Translational Sciences, National Institutes of Health, 9800 Medical Center Dr., MSC 3370, Bethesda, MD 20892-3370. Tel.: 301-827-6727; E-mail: wzheng@mail.nih.gov.

[3] The abbreviations used are: NPC, Niemann-Pick disease type C; α-T, α-tocopherol; δ-T, δ-tocopherol; BODIPY-LacCer, BODIPY-lactosylceramide; CLN2, ceroid lipofuscinosis, neuronal 2; GM2, GalNAcβ1,4(NeuAcα2,3)Galβ1,4Glcβ1Cer; GPN, Gly-Phe β-naphthylamide; LAL, lysosomal acid lipase; MPS IIIB, mucopolysaccharidosis type IIIB; BHK, baby hamster kidney; TRITC, tetramethylrhodamine isothiocyanate; HEXB, unpublished data.β-hexosaminidase.

body levels (6). Although the homeostasis of serum and tissue cholesterol has been well defined, many details of intracellular cholesterol regulation and trafficking are yet to be elucidated. Esterified cholesterol contained in low density lipoprotein (LDL) enters a cell via endocytosis. Upon LDL entry into the late endosome/lysosome, LAL hydrolyzes fatty acyl chains from cholesteryl esters to liberate unesterified cholesterol that is transported out of the late endosome/lysosome involving NPC1 and NPC2 proteins (6–8). The precise mechanism and pathway of cholesterol trafficking from the lysosome remain unclear, although it has been established that unesterified cholesterol moves to the endoplasmic reticulum for re-esterification or utilization by the cell and to the *trans*-Golgi network and/or plasma membrane for efflux from the cell (5, 9).

Currently, there are no Food and Drug Administration-approved therapies for either NPC disease or Wolman disease. However, miglustat, originally approved as a substrate reduction drug for Gaucher disease, has been approved in the European Union for the treatment of NPC1 disease by the European Agency for the Evaluation of Medicinal Products. Therapeutic strategies that have been explored include reduction of lysosomal lipid burden, augmentation of mutant protein expression, or replacement of mutant proteins in lysosome (10). Enzyme replacement therapy, which has been successfully used to treat selected lysosomal storage diseases, was studied in the mouse model of Wolman disease but is not clinically approved (11). A protein replacement therapy, similar to enzyme replacement therapy, would in theory be possible for NPC2 disease, but it is not feasible for NPC1 disease because NPC1 is an integral membrane protein. A phenotypic screen of a compound collection recently identified compounds that reduced filipin staining in NPC1 fibroblasts (12), and several laboratories have reported lead compounds, including 2-hydroxypropyl-β-cyclodextrin and histone deacetylase inhibitors, that reduce cholesterol accumulation (12–15). A recent report revealed that cyclodextrin's mechanism of action to reduce cholesterol accumulation in *NPC1* mutant cells is through induction of exocytosis (16). Here we report the identification of δ-tocopherol (δ-T) in a phenotypic screen of an approved drug library that significantly reduces lysosomal cholesterol accumulation in NPC1 fibroblasts. Following δ-T treatment, the enlarged acidic endosomal/lysosome compartment was dramatically reduced, and the pathological phenotype of NPC1 cells, as determined by ultrastructural analysis, was alleviated. Similar effects of δ-T were also observed in Wolman fibroblasts. The mechanism of action for δ-T was linked to increase in cytosolic Ca^{2+}, correction of the lysosomal Ca^{2+} deficiency, and enhancement of lysosomal exocytosis. The effect of δ-T also extended to patient-derived fibroblasts from other lysosomal storage diseases, including Batten (CLN2), Fabry, Farber, Niemann-Pick disease type A, NPC2, Sanfilippo type B (MPS IIIB), and Tay-Sachs. The results indicate that the enhancement of lysosomal exocytosis may represent a new therapeutic strategy for drug development that may be widely applicable to lysosomal storage diseases.

EXPERIMENTAL PROCEDURES

Materials—Hoechst and LysoTracker Red dye were purchased from Invitrogen. Filipin dye was obtained from Sigma-Aldrich. α-Tocopherol and δ-tocopherol were purchased from Sigma-Aldrich and purified by HPLC to a purity greater than 99%. β-Tocopherol (racemic), α-tocotrienol, β- tocotrienol, and γ-tocotrienol were obtained from Sigma-Aldrich in analytical standard grade (purity ≥97%). γ-Tocopherol and δ-tocotrienol were purchased from ChromaDex (Irvine, CA) in vitamin reference standard grade (purity >96%). The 96-well, 384-well, and 1536-well plates were purchased from Greiner Bio-One (Monroe, NC). Human skin fibroblast cell lines (supplemental Table S1) were purchased from the Coriell Cell Repository (Camden, NJ), including control cell line (GM05659), NPC1 (GM03123), NPC2 (GM17910), Wolman (GM11851), Batten (GM16485), Farber (GM20015), Fabry (GM00107), Niemann-Pick disease type A (GM16195), Sanfilippo type B (GM02552), and Tay-Sachs (GM00221). The GM03123 fibroblasts were utilized mainly in the NPC1 experiments unless specifically indicated. The NPC25 (c.2979dupA, p.N701K) skin fibroblast line was derived from an NPC1 patient evaluated under an NICHD, National Institutes of Health, Institutional Review Board-approved clinical protocol and obtained with consent.

Cell Culture—Both human fibroblasts and baby hamster kidney (BHK) cells were cultured in DMEM (Invitrogen, catalog no. 11995-040) supplemented with 10% fetal bovine serum (FBS), 100 unit/ml penicillin, and 100 μg/ml streptomycin in a humidified incubator with 5% CO_2 at 37 °C.

Approved Drug Collection—A collection of 2816 approved drugs that were dissolved in DMSO solution as 10 mM stock solution were set up as described previously (17). The compounds were serially diluted 1:5 in 384-well plates for seven concentrations and formatted into 1536-well plates at 5 μl/well as the compound source plates. In the primary screen, 23 nl of compounds in DMSO solution was transferred using a Pintool station (Klaypsys, San Diego, CA) to 1536-well assay plates containing 5 μl/well cell culture medium. The final concentrations of compounds ranged from 1.32 nM to 46 μM.

Amplex-Red Cholesterol Assay—Total cholesterol in patient cells was measured by the Amplex-Red cholesterol assay kit (Invitrogen). The unesterified cholesterol was determined using the same kit without the enzyme acid lipase. Esterified cholesterol was determined as the difference between the total and unesterified cholesterol values. The cells were seeded in black, tissue culture-treated 1536-well plates at 800 cells/well in 5 μl of medium by a Multidrop Combi dispenser (Thermo Scientific, Waltham, MA) and cultured for 24 h. The assay plates were added with 23 nl/well compound DMSO solution using a Pintool station (Klaypsys, San Diego, CA) and cultured for 3 days. The cells were washed twice using a centrifugation method in which the inverted plates were placed on a stack of paper towels and centrifuged at 800 rpm for 1 min followed by the addition of 7 μl/well PBS (added gently with a 45° angled liquid dispenser (Klaypsys)). The cholesterol assay mixture from the kit was added at 2.5 μl/well and incubated for 1 h at 37 °C. The resulting fluorescence intensity was measured with

excitation of 560 ± 10 nm and emission of 590 ± 10 nm in a fluorescence plate reader (Tecan, Durham, NC).

Cholesterol Analysis by Liquid Chromatography-Mass Spectrometry (LC-MS)—Cell pellets were collected from 100-mm dishes and washed once with 10 ml of PBS. Proteins were assayed using the BCA kit (Sigma-Aldrich), and lipids were extracted by a modified Bligh and Dyer procedure (18) from the cells. Internal standards were added based on protein concentration that included D7-cholesterol and 17:0 cholesteryl ester (Avanti Polar Lipids, Inc). The lipid extract was derivatized to convert cholesterol and its ester into acetate for facilitating ionization using a direct infusion mass spectrometric assay. The derivatization was performed by treating the dried crude lipid extract with solutions of 1 M acetic acid with 1 M DMAP (4-Dimethylaminopyridine) in chloroform and 1 M EDC (1-ethyl-3-(3-dimethylaminopropyl)-carbodiimide) in chloroform at 50 °C for 2 h. The derivatized product was extracted with hexane and analyzed by a direct infusion mass spectrometric assay with 5% ammonium hydroxide for facilitating ionization.

A triple-quadrupole mass spectrometer equipped with an electrospray was used for analysis of lipids in positive mode. Cholesterol and cholesteryl esters were detected by a neutral loss scan of 213 (collision energy, 50 V), neutral loss scan of 77 (collision energy, 14 V), and precursor ion scan of *m/z* 369 (collision energy, 14 V), respectively. Data processing of mass spectrometric analyses, including ion peak selection, data transfer, peak intensity comparison, and quantification, was conducted using self-programmed Microsoft Excel macros (19).

Cytotoxicity Assay—In an initial experiment, we found that commercially available vitamin E isoforms were cytotoxic at concentrations required for their pharmacological effect. The ATP content assay kit (Promega or PerkinElmer Life Sciences) was applied to monitor the compound cytotoxicity. Cells were seeded in white solid 96- or 1536-well plates and treated with compounds as described above for the cholesterol assay. On the day of the experiment, 3 μl/well assay mixture (prepared according to the manufacturer's instructions) was added to the assay plates, followed by incubation at room temperature for 10 min. The luminescence signal was determined in the luminescence mode of a Tecan multifunction plate reader.

Filipin Staining—Cells were seeded at 1500 cells/well in 100 μl of medium in black/clear bottom tissue culture-treated 96-well plates and cultured for 24 h. After the addition of compound solution, the plates were cultured for 3 days. The cells were washed twice with PBS and fixed by 100 μl/well 3.2% formaldehyde at room temperature for 30 min. After washing with PBS two times, the cells were stained with 100 μl/well 50 ng/ml filipin (freshly dissolved in DMSO at 10 mg/ml and then diluted in PBS) at room temperature for 1 h. The plates were stored at 4 °C after washing two times with PBS before the imaging analysis. On the day of the imaging experiment, cells were stained with 100 μl/well 2 μM CellMask-Red dye (Invitrogen, catalog no. H32711) in PBS at room temperature for 1 h. The plates were imaged using an Incell2000 automated fluorescence plate imaging reader (GE Healthcare) with a ×20 or ×40 objective. A DAPI filter set (excitation = 360 ± 20 nm, and emission = 460 ± 20 nm) and TRITC filter set (excitation = 545 ± 20 nm, and emission = 593 ± 20 nm) were used to visualize filipin and CellMask staining, respectively.

Nile Red Staining—The cells were cultured and treated as described above. On the day of the experiment, cells were washed two times with PBS and live-stained with 1 μM Nile Red dye solution (prepared in cell culture medium) at 100 μl/well, followed by an incubation at 37 °C for 10 min. After washing twice with PBS, the cells were fixed in 3.2% paraformaldehyde in PBS at 100 μl/well for 1 h at room temperature. The nuclear staining was carried out by an addition of 100 μl/well 1 μg/ml Hoechst 33342 (Invitrogen) in PBS and incubation at room temperature for 30 min. The plate was washed twice with PBS, and the images were measured in an Incell2000 imaging plate reader with an FITC filter set (excitation = 480 ± 20 nm, emission = 535 ± 36 nm) for the neutral lipids (cholesteryl esters and triglycerides) and a DAPI filter set for Hoechst nuclear staining.

BODIPY-lactosylceramide (BODIPY-LacCer) Staining—The cells in a 96-well assay plate were prepared as described above, incubated with 100 μl/well BODIPY-LacCer dye (Invitrogen, catalog no. B-34402) in 1% FBS DMEM, and incubated at 37 °C for 1 h, followed by plate washing with HEPES-buffered minimal essential medium (13.8 mM HEPES, 137 mM NaCl, 5.4 mM KCl, 2 mM glutamine, 0.4 mM KH_2PO_4, 0.18 mM Na_2HPO_4, 1× minimum essential medium vitamins, and 1× minimum essential medium amino acids at pH 7.4). The cells were rinsed with cold HEPES-buffered minimal essential medium containing 5% fatty acid-free BSA and back-exchanged at 11 °C six times over 60 min as described previously (20). Images were immediately taken in the InCell2000 imaging plate reader with the DAPI filter set.

LysoTracker Dye Staining—The assay was optimized to visualize the enlarged lysosomes by applying an appropriate concentration of LysoTracker dye in which the control cells exhibited minimal staining while the NPC1 or other disease cells showed significant staining. The cells were cultured and treated as described above. On the day of the experiment, cells were live-stained with 100 μl/well 50 nM LysoTracker Red DND-99 dye (Invitrogen, catalog no. L-7528) in medium at 37 °C for 1 h followed by plate washing twice with PBS. The plate was used for image analysis of live cell staining or was fixed in 100 μl/well 3.2% formaldehyde for 1 h and washed two times with PBS. The nuclear staining was performed by an addition of 100 μl/well 1 μg/ml Hoechst 33342 (Invitrogen) in PBS and incubation at room temperature for 30 min. After washing twice with PBS, the plates were stored at 4 °C until imaging analysis. A DAPI filter set and TRITC filter set in the Incell2000 imaging plate reader were used to visualize Hoechst nuclear staining and LysoTracker staining, respectively.

Electron Microscopy—Fibroblast cells were seeded in 6-well plates in 5 ml of medium at 150,000 cells/well and cultured for 1 day in the presence or absence of compounds. Cells were fixed in 2% glutaraldehyde, 0.1 M cacodylate buffer, pH 7.2, for 1 h at room temperature and then stored at 4 °C until transmission electron microscopy analysis was performed. The cells were postfixed in 1% osmium tetroxide in the same buffer for 1 h and stained en bloc with 0.5% uranyl acetate in 0.1 M acetate buffer, pH 4.2. The cells were then dehydrated in graded ethanol solu-

tions (35, 50, 70, 95, and 100%) and infiltrated overnight in epoxy resin (Poly/Bed 812, Polysciences). After adding fresh pure resin, the cell plates were cured for 72 h in 55 °C. After removing the polystyrene plates, suitable areas for thin sectioning were selected, cut out with a jewelry saw, and glued onto empty resin stubs. About 70-nm thin sections were cut on an ultramicrotome (Leica EM UC6) and mounted on naked copper grids. The thin sections were double-stained (uranyl acetate and lead citrate) and examined in a Hitachi H-7650 transmission electron microscope, and images were taken using an AMT CCD camera (21).

Western Blot Analysis—Cell lysates were prepared, and protein concentrations were determined as described above. Samples were heated at 65 °C for 10 min before being resolved by SDS-PAGE under reducing conditions. Proteins were transferred to PVDF membranes (Bio-Rad) using either Criterion Blotter (Bio-Rad) or iBlot dry blotting devices (Invitrogen). For NPC1 and 3-hydroxy-3-methylglutaryl-CoA reductase detection, rabbit polyclonal antibodies against NPC1 (Abcam, catalog no. ab36983; 1:2000) or 3-hydroxy-3-methylglutaryl-CoA reductase (Millipore, catalog no. 07-457; 1:1000) were used, respectively. A peroxidase-conjugated donkey anti-rabbit IgG (Santa Cruz Biotechnology, Inc.) was used as secondary antibody at a 1:500 dilution. Flotillin, an exosome marker, was determined using a method described previously (16). Briefly, the media from cells in 100 × 20-mm dishes treated with 40 μM δ-T or two positive controls (2% 2-hydroxypropyl-β-cyclodextrin and 1 μM ionomycin) for 1 h at 37 °C were collected and centrifuged at 100,000 × *g* for 1 h for isolation of exosomes. The resulting exosomes were resuspended in 20 mM Tris-HCl buffer (pH 8.0) and sonicated in a bath sonicator to yield the final samples for Western blot analysis as described above. A mouse anti-flotillin 2 antibody (BD Biosciences) was used for the detection of flotillin in the exosomes. Cells were lysed, and the cell lysates were collected for the determination of GAPDH used for normalization of proteins in each sample.

[^{3}H]Cholesterol Efflux Assay—Efflux of cholesterol from BHK cells was performed as described previously (22). Briefly, BHK cells and BHK cells stably transformed with ABCA1, ABCG1, and Scavenger receptor type B class I (SR-BI) were radiolabeled with [^{3}H]cholesterol (1 μCi/ml) in medium for 24 h. After washing three times with DMEM, DMEM containing 50 μg/ml HDL was added and cultured for 18 h. The radioactivity in the HDL-containing medium and cell lysate were determined. The percentage of total radiolabeled cholesterol effluxed into the medium was calculated by dividing by the sum of the radioactive counts remaining in the cells after the efflux period plus the counts in medium.

Intracellular and Lysosomal Ca^{2+} Measurements—Intracellular cytosolic Ca^{2+} concentration was measured fluorescently using a Fluo-8 dye kit (ATT Bioquest, Sunnyvale, CA) as described previously. Briefly, fibroblasts were cultured at 2500 cell/well in 20 μl of medium in black/clear bottom 384-well plates for 24 h at 37 °C. The calcium dye mixture was added at 20 μl/well and incubated at 37 °C for 30 min followed by room temperature for 30 min. The plates were then placed into a fluorescence kinetic plate reader (μCell, Hamamatsu, Hamamatsu City, Japan). The basal fluorescence intensity was recorded 10 times at 1 Hz for 10 s, and the compound (δ-T or α-T) was then added at 20 μl/well inside the instrument followed by an additional reading at 1 Hz for 5 min. The results were normalized to the average basal fluorescence intensity in a ratio, and the peak response (maximum) was used for the result calculation. The lysosomal Ca^{2+} induced by Gly-Phe β-naphthylamide (GPN) was measured similarly as that for cytosolic Ca^{2+}, except 200 nM GPN was added instead of δ-T or α-T after the measurement of basal fluorescence intensity that released lysosomal Ca^{2+}.

Endocytosis and Lysosomal pH Measurement—Endocytosis was measured using a fluorescence-labeled dextran dye (pHrodo™ dextran; catalogue no. P10361, Invitrogen) that enters cells through endocytosis. This dye emits fluorescent signal at the acidic pH while exhibiting a minimal fluorescence signal at neutral pH. The fibroblasts in 96-well plates were treated with 40 μM δ-T or 80 μM α-T for 24 h and incubated with 20 mg/ml pHrodo dye for 16 h. The live cell imaging was carried out after a cell wash with PBS with an excitation of 560 nm and emission of 590 nm. Chlorpromazine, a known inhibitor of endocytosis, was used as a positive control (final concentration of 5 μg/ml). The lysosomal pH was determined using a fluorescent LysoSensor dextran dye (catalogue no. L-22460, Invitrogen) that emits strongly at 530 nm in an acidic pH environment and at 450 nm in neutral pH. The fibroblasts in 96-well plates were treated with 40 μM δ-T for 24 h and incubated with the pH indicator dye for 16 h. The images were taken using Incell2000 (GE Healthcare) with an excitation of 360 nm, emission-1 of 530, and emission-2 of 450 nm.

Measurement of β-Hexosaminidase (HEXB) Release—Fibroblasts were cultured in 24-well plates at 30,000 cells/well in 0.4 ml of medium for 1 day at 37 °C. After being washed twice with assay buffer (DMEM with 2 mM D-mannose 6-phosphate sodium salt), the cells with 0.4 ml/well assay buffer were incubated at 37 °C with 0.2 ml/well compound in assay buffer. At the 5, 10, 20, 30, and 40 min time points, 30 μl of assay buffer from each well in the 24-well plate were aliquoted into a 96-well black plate. The rest of the assay buffer in the 24-well plate was discarded, followed by the addition of 0.6 ml of 1% Triton X-100 in distilled H_2O to lyse the cells. After incubation at 37 °C for 30 min, 6 μl/well cell lysate were added to the 96-well plate with 24 μl of assay buffer, followed by 90 μl/well 2.25 mM HEXB substrate, 4-methylumbelliferyl *N*-acetyl-β-D-glucosaminide (Sigma-Aldrich, catalog no. M2133), in a 25 mM citric acid buffer at pH 4.5. The 96-well plate was then measured in the Tecan fluorescence plate reader (excitation = 365 ± 20 nm, and emission = 460 ± 20 nm) after a 1-h incubation at 37 °C and the addition of 100 μl/well stop solution (1 M glycine and 1 M NaOH at pH 10.5).

Data Analysis and Statistical Analysis—The compound library screen data were analyzed using software developed internally at the National Institutes of Health Chemical Genomics Center. Concentration-response curves were analyzed, and EC_{50} values (mean ± S.D.) were calculated using Prism software (GraphPad, Inc., San Diego, CA). Results in figures are expressed as the mean of triplicates ± S.D. The statistical significance of differences was determined by a two-tailed

A.

Name	Structure	EC_{50} (μ M) (NPC1 cells)	EC_{50} (μ M) (Wolman cells)
α-Tocopherol	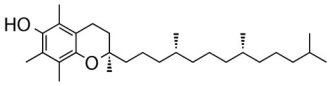	42.9 ± 1.3	28.7 ± 7.2
β-Tocopherol[a]	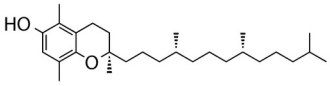	58.6 ± 5.1	36.1 ± 4.9
γ-Tocopherol	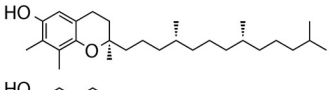	33.4 ± 6.5	17.2 ± 3.7
δ-Tocopherol	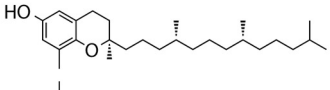	13.2 ± 2.7	9.0 ± 2.6
α-Tocotrienol	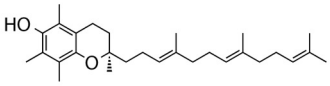	36.0 ± 5.8	30.1 ± 4.4
β-Tocotrienol	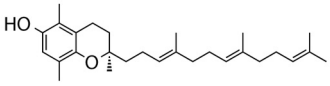	27.7 ± 6.4	19.9 ± 2.7
γ-Tocotrienol	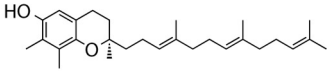	23.9 ± 3.8	16.3 ± 4.3
δ-Tocotrienol	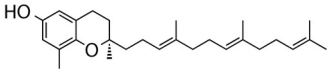	13.8 ± 1.8	10.4 ± 1.8

[a] Racemic version of β-Tocopherol was used in this study.

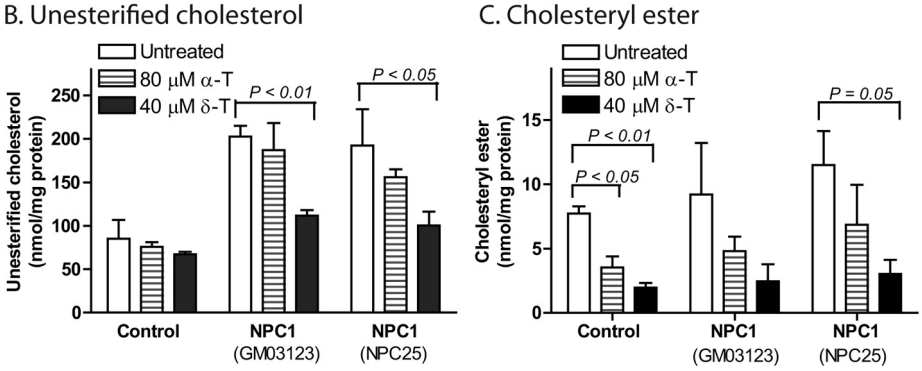

FIGURE 1. **Chemical structures of eight isoforms of vitamin E and EC_{50} values for reduction of cholesterol accumulation in NPC1 and Wolman fibroblasts.** *A*, the difference between tocotrienols and tocopherols is that tocotrienols have three double bonds in the phytyl side chain, whereas tocopherols do not. The EC_{50} values in NPC1 fibroblasts were measured for the reduction of cellular unesterified cholesterol, whereas the EC_{50} values in Wolman fibroblasts were determined for the reduction of total cellular cholesterol (unesterified cholesterol and cholesteryl ester). Cellular unesterified cholesterol (*B*) and cellular cholesteryl ester (*C*) were decreased by 40 μM δ-T or 80 μM α-T in two NPC1 cell lines (GM03123 and NPC25) measured by the LC-MS method. Results are showed as the mean of three experiments with S.D. (*error bars*).

single-factor analysis or variance or Student's *t* test. A *p* value of $\leq$0.05 was considered significant.

RESULTS

High Throughput Screen and Identification of Cholesterol Reduction Activity of δ-T—Skin fibroblasts derived from NPC1 patients demonstrate profound and reproducible cholesterol accumulation in late endosomes and lysosomes and, therefore, provide a robust cellular model of NPC1 disease (12, 16). Using a phenotypic screen of 2816 approved drugs with a biochemical assay to measure unesterified cholesterol, δ-T was identified as a lead compound that dramatically reduced cellular cholesterol accumulation in NPC1 fibroblasts. δ-T is one of eight components in natural vitamin E that consists of a mixture of four tocopherols and four tocotrienols. All eight isoforms reduced unesterified cholesterol accumulation in a concentration-dependent manner with EC_{50} values ranging from 13.2 μM for δ-T to 58.6 μM for β-tocopherol (Fig. 1*A*). A similar reduction of cholesterol accumulation was observed in NPC2 fibroblasts (supplemental Fig. S1*A*). Cholesterol accumulation in NPC1 fibroblasts was not affected by lovastatin, an inhibitor of cellular cholesterol synthesis; by either vitamin C or *N*-acetylcysteine, classical antioxidants; or by vitamin K, one of the other lipid soluble vitamins (supplemental Fig. S1*B*). The cholesterol-reducing effect of δ-T in NPC1 cells was confirmed by LC-MS analysis (Fig. 1*B*). In addition to the reduction of unesterified cholesterol, cholesteryl esters were also reduced in the NPC1 cells after the treatment with δ-T (Fig. 1*C*). To assess the spec-

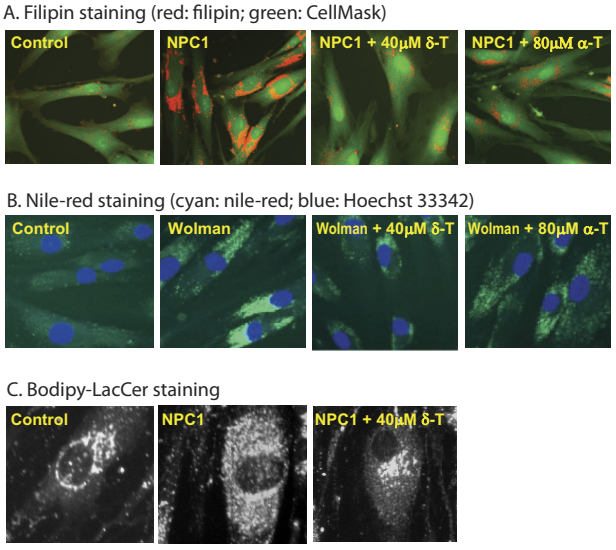

FIGURE 2. **δ-T and α-T reduced cholesterol accumulation phenotypes in NPC1 and Wolman fibroblasts.** Filipin staining of unesterified cholesterol was reduced in NPC1 cells (*A*), and Nile Red staining of neutral lipids (cholesteryl ester and triglyceride) was decreased in Wolman fibroblasts (*B*) by 40 μM δ-T or 80 μM α-T. The filipin-stained cells were co-stained with CellMask, a plasma membrane dye. *C*, mistrafficking of BODIPY-LacCer in NPC1 fibroblasts was corrected by 40 μM δ-T.

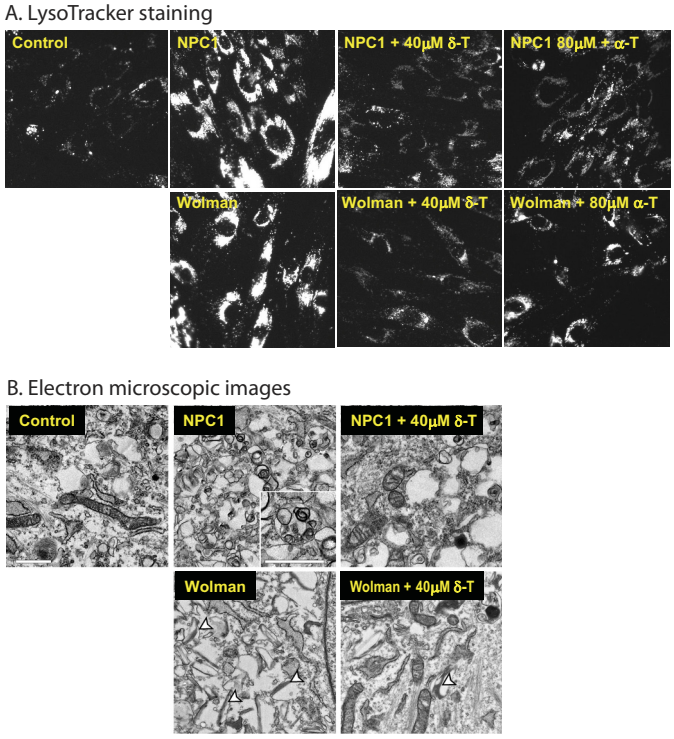

FIGURE 3. **δ-T and α-T reduced cellular acidic compartments and decreased pathological lysosomal inclusions in NPC1 and Wolman cells.** *A*, the LysoTracker dye staining (for acidic compartments) was reduced in both NPC1 and Wolman cells by 40 μM δ-T or 80 μM α-T. The LysoTracker Red staining images were merged with Hoechst nuclei dye staining. *B*, electron micrographs of thin sections of NPC1 and Wolman fibroblasts were compared with control fibroblasts. The *inset* in the untreated NPC1 fibroblast shows in detail the lamellated and osmophilic structures in lysosomes (*bar*, 1 μm) that were significantly reduced by the treatment with 40 μM δ-T. In the untreated Wolman fibroblasts, the *white arrowheads* mark the typical elongated and cleft-shaped lipid droplets in lysosomes that were alleviated after the treatment with 40 μM δ-T.

ificity of δ-T to reduce cholesterol accumulation, we tested δ-T in Wolman fibroblasts. Wolman fibroblasts have significantly decreased levels of LAL activity and accumulate cholesteryl ester in lysosomes. We found that δ-T effectively reduced total cholesterol, including cholesteryl ester. δ-T was the most potent (EC_{50} = 9.0 μM) one among the vitamin E isoforms in the Wolman fibroblasts (Fig. 1*A*). We also found that all of the vitamin E isoforms exhibited no cytotoxicity up to 80 μM in the treatment of control and patient cells for 4 days except for γ-tocotrienol and δ-tocotrienol, which showed cytotoxicity at 80 μM (supplemental Fig. S2).

δ-T Reduces Lysosomal Size and Corrects Ultrastructural Pathology of NPC1 and Wolman Cells—Filipin is a fluorescent antibiotic that binds to unesterified cholesterol and is commonly used in the diagnosis of NPC1 disease (12, 16, 23). Treatment of NPC1 fibroblasts with either 40 μM δ-T or 80 μM α-T significantly reduced unesterified cholesterol storage (Fig. 2*A*), a cellular phenotypic hallmark of NPC1 disease, thus confirming the biochemical findings. Likewise, treatment of Wolman cells with these two compounds significantly reduced staining with Nile Red (Fig. 2*B*), a dye used to detect nonpolar lipids, including cholesteryl ester and triglyceride (24), consistent with the observed reduction of cholesteryl ester accumulation. In addition to accumulation of unesterified cholesterol, NPC1 fibroblasts exhibit lysosomal storage of other lipids, including lactosylceramide (20). Thus, we examined whether the altered trafficking of a fluorescent lactosylceramide analog, BODIPY-LacCer, could be corrected by δ-T treatment. After treatment with 40 μM δ-T, BODIPY-LacCer staining in the NPC1 fibroblasts was dramatically reduced, approaching normal levels (Fig. 2*C*). These results suggest that the reduction of lysosomal cholesterol accumulation by δ-T may also help to correct the defective trafficking of other lipids in NPC1 cells.

The mixed lipid storage phenotype results in a marked enlargement of lysosomes in the NPC1 and Wolman fibroblasts. Therefore, we next determined whether the enlarged lysosomes in these cells could be reduced by the treatment with δ-T. LysoTracker, a probe that stains the intracellular acidic compartment, has been used to visualize the enlarged endolysosomal compartment in NPC1 cells (20). We found increased LysoTracker staining in both NPC1 and Wolman fibroblasts, as expected. Treatment with either 40 μM δ-T or 80 μM α-T significantly reduced LysoTracker staining in both types of fibroblasts (Fig. 3*A*). Both NPC1 and Wolman fibroblasts have a distinct ultrastructural phenotype that is evident by electron microscopy (25, 26). The electron microscopic images exhibited enlarged lysosomes full of lamellated membranes and dense osmiophilic material in NPC1 cells and lipid droplet-like and cleft-like lysosomes in Wolman cells (Fig. 3*B*). Treatment with 40 μM δ-T significantly reduced the characteristic storage materials in lysosomes of both cell types. Together, these findings demonstrate that the δ-T-mediated cholesterol reduction is associated with alleviation of the disease phenotypes in NPC1 and Wolman cells.

δ-T Increases [^{3}H] Cholesterol Efflux—To investigate the mechanism of action of δ-T, we analyzed its effect on the expression of the NPC1 protein and other proteins involved in cholesterol homeostasis. We found that the protein levels of

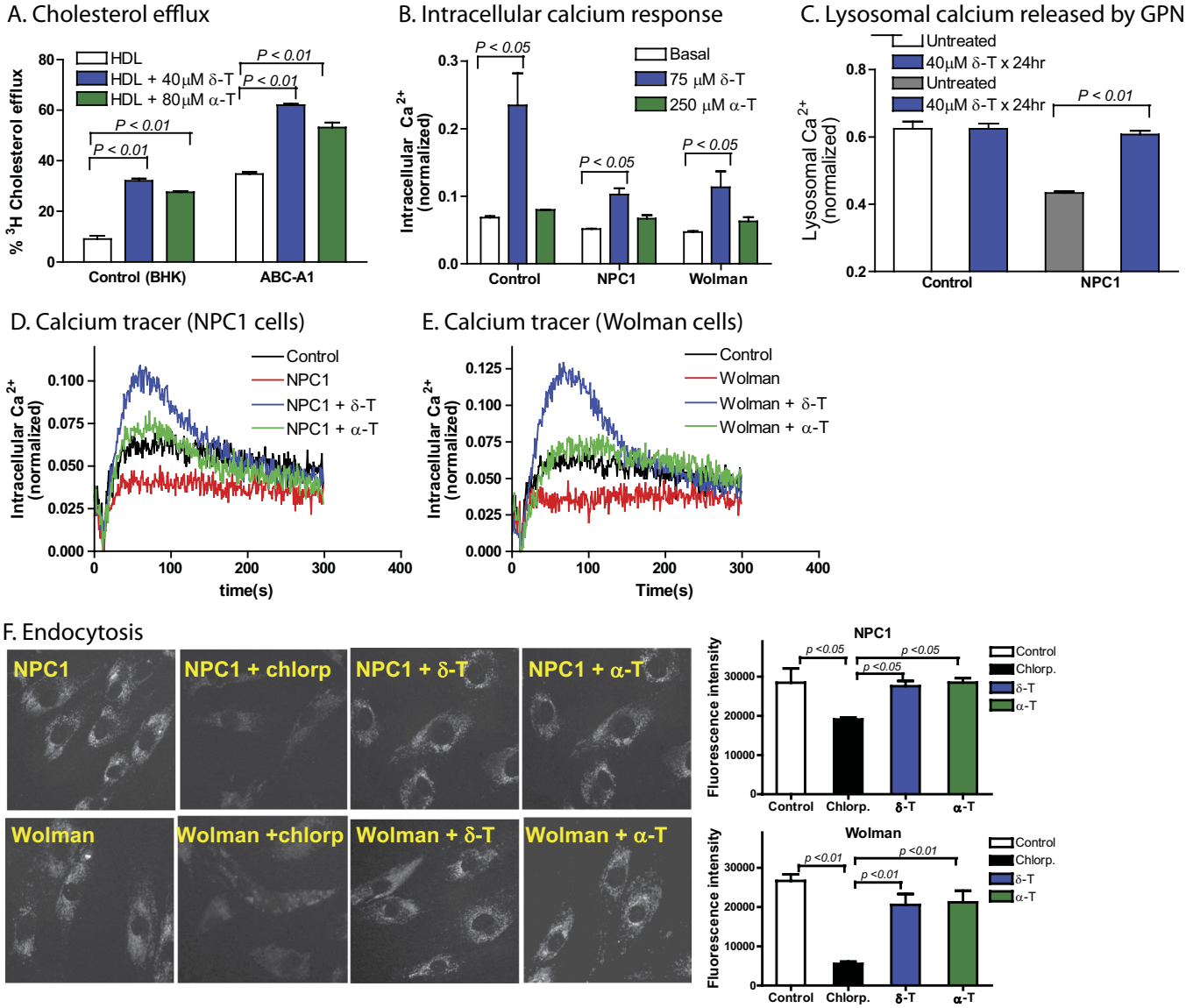

FIGURE 4. **δ-T increased cholesterol efflux and intracellular Ca^{2+} concentration.** *A*, [^{3}H]cholesterol efflux carried out by the addition of HDL in medium was enhanced by 40 μM δ-T and 80 μM α-T in the BHK cells, respectively. The efflux of [^{3}H]cholesterol was greatly augmented by the expression of ABCA1 transporters in BHK cells, which was further enhanced by δ-T and α-T. *B*, intracellular Ca^{2+} increased in the presence of 75 μM δ-T or 250 μM δ-T in both NPC1 (see *D* for the calcium tracers) and Wolman (see *E* for the calcium tracers) fibroblasts. *C*, δ-T reduced the impairment of lysosomal Ca^{2+} release in NPC1 cells. The NPC1 fibroblasts exhibited reduced lysosomal Ca^{2+} release stimulated by 200 nM GPN, which was partially corrected by a 24-h pretreatment with 40 μM δ-T. Results shown are the mean of three experiments; *error bars* represent S.D. *F*, images of endocytic vesicles indicated by a fluorescent pHrodo™ dextran dye in NPC1 and Wolman fibroblasts. Chlorpromazine (*Chlorp*) (a known inhibitor of endocytosis) was used as a positive control. The treatment with 40 μM δ-T or 80 μM α-T did not alter the fluorescence intensity in the endocytic vesicles in these cells, indicating that both compounds do not affect the endocytosis in NPC1 and Wolman fibroblasts.

NPC1, 3-hydroxy-3-methylglutaryl-CoA reductase (the rate-limiting enzyme in cholesterol synthesis), and ABCA1 (a sterol transporter) were also not altered by δ-T treatment in NPC1 fibroblasts (supplemental Fig. S4). Taken together, these data indicate that the effect of δ-T is probably not mediated by a change in either *de novo* cholesterol synthesis or the major transporter involved in cholesterol efflux.

We then examined the effect of tocopherol on [^{3}H]cholesterol efflux in BHK cells that express ABCA1 at basal level and a BHK cell line with overexpression of ABCA1. We found that 40 μM δ-T or 80 μM α-T increased the efflux of [^{3}H]cholesterol in BHK cells from 9.0% to 32.1 or 27.6%, respectively (Fig. 4*A*). In the ABCA1-overexpressing cells, [^{3}H]cholesterol efflux at the basal level was much higher than that in the parental cells. Treatment with 40 μM δ-T or 80 μM α-T was able to further increase [^{3}H]cholesterol efflux in the ABCA1-overexpressing cells (Fig. 4*A*). A similar increase in [^{3}H]cholesterol efflux was also observed in cells overexpressing ABCG1 and SR-B1 (supplemental Fig. S5). These results suggest that increased cholesterol efflux by δ-T may not be mediated by activation of a specific cholesterol efflux pathway but rather by increasing the general cholesterol efflux through diverse cellular pathways (27).

δ-T Increases Intracellular Ca^{2+} Concentration and Ameliorates Lysosomal Calcium Deficiency in NPC1 Cells—Increase in the concentration of intracellular Ca^{2+}, an important second messenger, triggers a variety of cellular responses, including

lysosomal exocytosis. In NPC1 fibroblasts, there is a dysregulation of calcium homeostasis, as evidenced by lysosomal Ca^{2+} deficiency (20). Treatments that compensate for loss of lysosomal Ca^{2+} (*e.g.* curcumin) have been reported to reduce cholesterol storage in NPC1 cells (20). To explore whether δ-T may similarly exert its effects through changes in intracellular Ca^{2+}, we measured cytosolic calcium levels in both NPC1 and Wolman cells following the treatment with δ-T. We found that δ-T stimulated a transient increase of cytosolic Ca^{2+} in both NPC1 and Wolman fibroblasts as well as in control fibroblasts (Fig. 4, *B*, *D*, and *E*). In addition, the intracellular Ca^{2+} response to δ-T was independent of extracellular Ca^{2+} concentration (supplemental Fig. S6*A*), indicating that Ca^{2+} was released from intracellular storage sites, such as the endoplasmic reticulum, in response to δ-T. We further studied the effect of δ-T on lysosomal Ca^{2+} released by GPN in NPC1 fibroblasts. Consistent with an earlier report (20), lysosomal Ca^{2+} was reduced in NPC1 cells compared with that in control cells. Treatment of NPC1 fibroblasts with 40 μM δ-T for 24 h significantly increased lysosomal Ca^{2+} (Fig. 4*C*), and this effect was not dependent on extracellular Ca^{2+} (supplemental Fig. S6*B*).

To examine the potential effect of δ-T on the endocytosis, we treated the fibroblasts with a fluorescent dextran dye that enters the cells via endocytosis and becomes fluorescent in acidic compartments. We found that the treatment with δ-T did not alter the fluorescence intensity of this dye in the endocytic vesicles in both NPC1 and Wolman cells (Fig. 4*F*), indicating that δ-T does not affect the endocytosis. We also measured the pH in late endosomes and lysosomes using a fluorescent pH indicator dye. The treatment with δ-T in the fibroblasts did not change the fluorescence intensity of this pH dye staining in acidic compartments (supplemental Fig. S3), suggesting that δ-T does not affect the pH in late endosomes and lysosomes.

δ-T Stimulates Lysosomal Exocytosis in NPC1 and Wolman Fibroblasts—2-Hydroxypropyl-β-cyclodextrin has been reported to promote a calcium-dependent lysosomal exocytosis, which offers a potential mechanism for its cholesterol-reducing effect in NPC1 fibroblasts (16). We measured lysosomal exocytosis in δ-T-treated NPC1 and Wolman fibroblasts by determining the activity of HEXB, a lysosomal enzyme, in the extracellular medium. We found that HEXB activity increased in culture medium after 40 μM δ-T treatment for 24 h compared with the vehicle-treated cells (Fig. 5, *A–C*). The increased HEXB activity in culture medium stimulated by the 24-h incubation with δ-T exhibited kinetics and extent of enzyme release different from those induced by the calcium ionophore ionomycin (supplemental Fig. S7, *A–C*). The basal levels of HEXB activity in the culture medium were also higher in the NPC1 and Wolman fibroblasts compared with that in the wild type cells (supplemental Fig. S7*D*). We then determined the effect of δ-T on the secretion of flotillin 2, an exosome marker, whose secretion was increased by 2-hydroxypropyl-β-cyclodextrin and ionomycin in fibroblasts (16). Treatment with δ-T stimulated the secretion of flotillin 2 (Fig. 5*D*), indicative of release of the vesicles derived from endolysosomes. We also observed in the electron microscopic images a tendency for the stored materials (in endosomal and lysosomal compartments) to be distributed closer to the plasma membrane and more distant from the nucleus in addition to a reduction in the amount of stored materials after treatment with 40 μM δ-T (Fig. 5*E*). Taken together, these results demonstrate that the pharmacological effect of δ-T may be mediated by the increase of cytosolic Ca^{2+} and enhancement of lysosomal exocytosis.

δ-T Reduces Lipid Storage and Lysosomal Enlargement in Fibroblasts from Patients with Other Lysosomal Storage Diseases—Lipid accumulation in the lysosome and enlargement of lysosome size in affected cells are common features of more than 50 lysosomal storage diseases caused by genetic mutations of genes generally encoding lysosomal proteins (28). Despite the heterogeneity in cellular phenotypes among these diseases, lysosomal exocytosis has recently emerged as a new drug target for the potential treatment of these storage disorders (29, 30). Based on the data for both NPC1 and Wolman cells, we hypothesized that the pharmacological effect of δ-T on the intracellular Ca^{2+} and lysosomal exocytosis is a general mechanism for elimination of lysosomal storage. To test this hypothesis, we measured the ability of δ-T to decrease acidic/lysosomal compartment size as determined by LysoTracker staining in fibroblasts derived from patients with six other diseases. Lysosomal storage in these fibroblasts consists of ceroid/lipofuscin in Batten (CLN2), globotriaosylceramide in Fabry, ceramide in Farber, sphingomyelin in Niemann-Pick disease type A, partially degraded heparan sulfate in Sanfilippo type B, and GM2 ganglioside in Tay-Sachs (supplemental Table S1). Whereas untreated fibroblasts showed increased LysoTracker staining, indicating the enlarged lysosomes (Fig. 6, *A* and *B*), treatment with 40 μM δ-T significantly reduced the LysoTracker staining in all six fibroblast cell lines studied (Fig. 6, *A* and *B*). The reduction of acidic cellular compartments by δ-T treatment is consistent with decreased intracellular storage that was confirmed by alleviation of the ultrastructural pathology (Fig. 6, *C* and *D*). Thus, the amelioration of lysosomal pathology by δ-T, initially demonstrated in NPC1 and Wolman cells, can be generalized to other lysosomal storage diseases.

DISCUSSION

Exocytosis is a housekeeping function responsible for the secretion of hormones, cytokines, and neurotransmitter in secretory cells. In response to a transient increase of cytosolic Ca^{2+}, secretory vesicles move toward the plasma membrane, fuse with the membrane, and then expel the luminal contents into the external cellular environment. Exocytosis in nonsecretory cells plays an important role in plasma membrane repair (31), bone resorption (30), cycling/recycling proteins to plasma membrane (32), pathogen invasion (33), neurite outgrowth (34), and cellular clearance (29, 35). Lysosomes, which are the most important exocytic organelle in nonsecretory cells, release their contents in response to a transient rise in cytosolic Ca^{2+} or ionomycin (29). A recent paper reported that lysosomal exocytosis is regulated by the bHLH-leucine zipper transcription factor EB, and overexpression of transcription factor EB reduces the storage materials in cell-based disease models (30). Regulated exocytosis may be operative *in vivo* because lysosomal contents have been found in extracellular fluids, blood, and urine in certain patients with lysosomal storage diseases

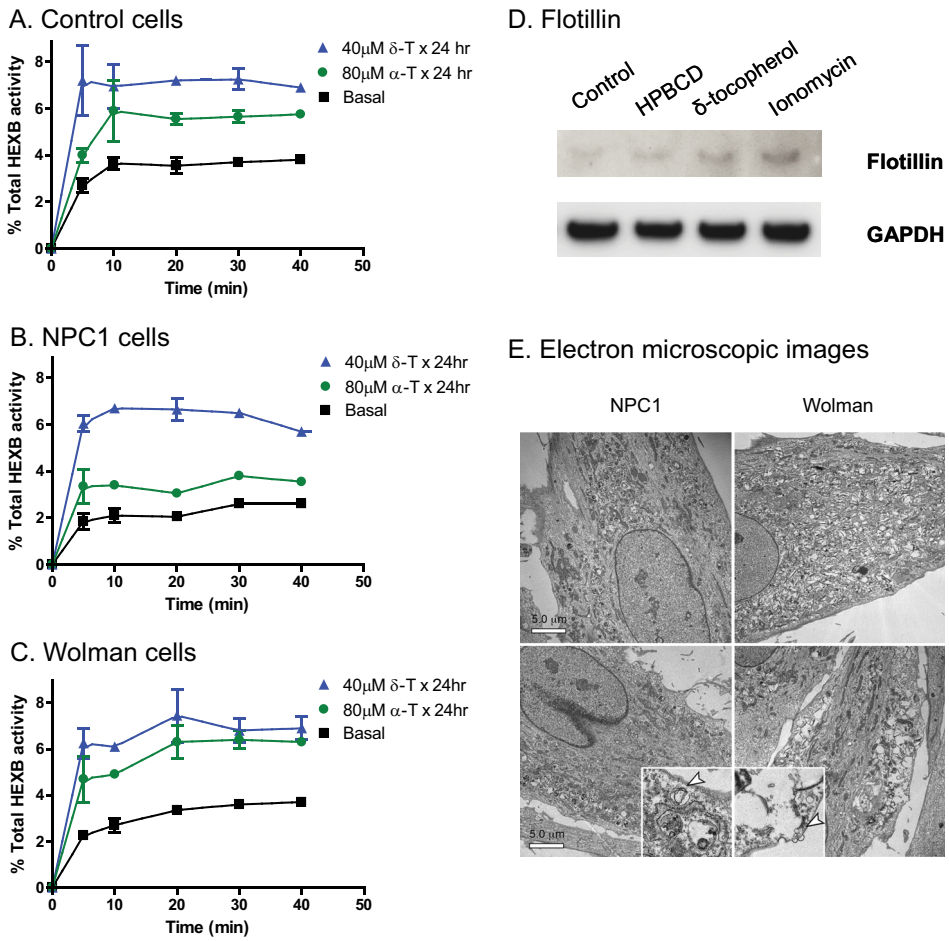

FIGURE 5. **Lysosomal exocytosis in δ-T- and α-T-treated NPC1 and Wolman disease fibroblasts.** Lysosomal exocytosis was enhanced by δ-T and α-T in NPC1 (*A*) and Wolman (*B*) fibroblasts as well as in the control fibroblasts (*C*). After a 24-h pretreatment with 40 μM δ-T or 80 μM α-T, the activity of HEXB (a lysosomal enzyme) in extracellular medium significantly increased in all three cell types. The data shown are the mean of three experiments, and the *error bars* represent S.D. *D*, secretion of exosomes in δ-tocopherol-treated cells measured by Western blot analysis of flotillin 2 in the culture medium of control fibroblasts. The *top panel* exhibits the bands detected by an anti-flotillin 2 antibody in exosome fractions incubated with buffer, 2% 2-hydroxypropyl-β-cyclodextrin (a positive control), 160 μM δ-tocopherol, or 1 μM ionomycin. Equal loading was normalized by GAPDH levels in the cell lysate (*bottom panel*). *E*, electron micrographs of untreated NPC1 (*top left*) and Wolman (*top right*) cells *versus* treated NPC1 (*bottom left*) and Wolman (*bottom right*) cells show that the lysosomal storage materials in 40 μM δ-T not only decreased but also moved closer to the plasma membrane in overall distribution in the cell (*bar*, 5 μm). *Insets*, ×5 magnified areas with vesicles close to the plasma membrane.

(35). Thus, targeting lysosomal exocytosis may be a useful strategy to mitigate the lysosomal burden in storage diseases.

In this study, we show that δ-T, a minor vitamin E species, appears to exert its effect in NPC1 and Wolman fibroblasts through stimulation of lysosomal exocytosis. Translating these cell-based results to the *in vivo* use in animal models and patients poses a challenge with respect to its unfavorable pharmacokinetics. In comparison with α-T, which is present at 20–40 μM in human plasma, the highest among eight vitamin E isoforms, the δ-T plasma concentration in humans is <1 μM (36–39). Contributing to the low plasma concentration of δ-T is its rapid oxidation by the P450 enzyme CYP4F2 (40). The brain concentration of δ-T in mice was under 1 μM after a 4-week treatment with 1.67 g/kg of diet/day δ-T (49). By contrast, α-T, unique among the vitamin E isoforms, is stabilized in plasma by α-tocopherol transfer protein (41). Nonetheless, α-T is far less potent than δ-T in reducing storage in NPC1 and Wolman fibroblasts and, even with a dietary supplement, may not reach the required plasma concentration for this pharmacological effect (36, 38). In the *Npc1*$^{-/-}$ mouse model, treatment with α-T provided a functional benefit, although it did not prolong survival (42). This could be due to low plasma and tissue concentrations of α-T in the mouse that are insufficient for the activity of cholesterol reduction. Therefore, the insufficient therapeutic concentrations in plasma and brain limit the use of δ-T and α-T in the animal model study as well as in clinical use to treat patients. To explore the potential effect of δ-T *in vivo*, chemical optimization of its pharmacokinetic properties will be required.

Although the antioxidant capacity of vitamin E is frequently thought to be its primary biological function, a number of non-antioxidant functions have been proposed. These include regulation of enzyme function, cell signaling, cell proliferation, and neuroprotection (43, 44). Vitamin E contains a chromanol ring with a hydroxyl group that is responsible for its antioxidant effect and a 13-carbon hydrophobic phytyl side chain that inserts into the plasma membrane (45). α-T, the major vitamin E isoform in human plasma, prevents apoptosis induced by 7-ketocholesterol, one of the cholesterol oxidation products in neuronal cells that is markedly increased in NPC1 disease (46).

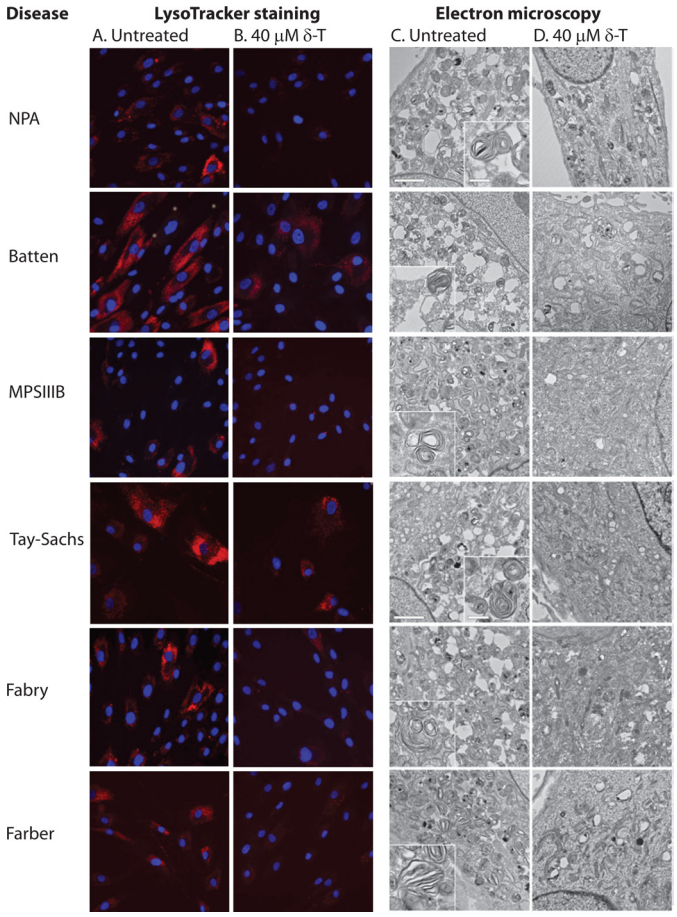

FIGURE 6. **Effect of δ-T on ultrastructural pathology in lysosomal storage disorder fibroblasts.** Treatment with 40 μM δ-T reduced lysosomal size and corrected lysosomal inclusions in patient fibroblasts of Batten (CLN2), Fabry, Farber, Niemann-Pick disease type A, Sanfilippo type B (MPS IIIB), and Tay-Sachs diseases. Shown are images of LysoTracker staining in the absence (*A*) or presence (*B*) of 40 μM δ-T treatment. LysoTracker Red staining was significantly reduced after the treatment with δ-T, consistent with a decrease of the acidic compartment size. Electron micrographs of patient fibroblasts in the absence (*C*) or presence (*D*) of δ-T (*bar*, 2 μm in the *main panels* and 500 nm in the *insets*). Typical large osmiophilic, mono- and multinuclear multilamellar bodies are observed in Niemann-Pick disease type A (*NPA*), Tay-Sachs, and Farber disease cells; similar but smaller and usually multinuclear multilamellar bodies are observed in Batten (CLN2), Sanfilippo type B (MPS IIIB), and Fabry disease cells (see *insets* for detail). The pathological phenotypes in the ultrastructure were significantly alleviated after the treatment with 40 μM δ-T in all of these six types of patient fibroblasts.

α-T has also been shown to stimulate mast cell degranulation, a secretory form of exocytosis (47). This effect of α-T was not mediated by an up-regulation of genes for proteins involved in vesicular transport (*e.g.* Nsf, Cplx2, Snap23, and Stx3) but through the direct interaction of α-T with the plasma membrane (47). The pretreatment requirement of α-T for these reported pharmacological effects may be explained by the time necessary for the incorporation of α-T molecules into the plasma membrane and for the subsequent transfer of incorporated α-T molecules to other cellular organelles and compartments.

A specific target protein for δ-T has not been found or implicated. In lysosomal storage diseases, the accumulation of lipids in lysosomes impairs cellular lipid trafficking, which could directly impact plasma membrane fluidity and dynamics. It is possible that the incorporation of δ-T in the plasma membrane and the subsequent alteration of membrane physical status, such as lipid fluidity, plays a critical role in the effect of δ-T on reduction of cholesterol and other lipid in the lysosome. The increase of intracellular Ca^{2+} and subsequent lysosomal exocytosis by δ-T support a mechanism of action mediated through the favorable change in membrane physical status. Thus, further studies on membrane biophysics and the function of membrane protein as affected by δ-T are necessary to elucidate the precise mechanism of action.

Based on the above data, we have proposed a model for the pharmacological effect of δ-T on the reduction of lipid accumulation in cells from patients with lysosomal storage diseases. Under normal conditions, cellular cholesterol derived from either LDL endocytosis or *de novo* synthesis is mobilized from lysosomes through a LAL-NPC2-NPC1-dependent pathway for distribution to the *trans*-Golgi and endoplasmic reticulum. We hypothesized that a minor, low flux cholesterol trafficking pathway, such as lysosomal exocytosis, may also exist because the cholesterol accumulation in NPC1 cells can be corrected following culture in lipoprotein-deficient serum for 5–6 days (48). Deficiency in function of the NPC1 protein disrupts the LAL-NPC2-NPC1-dependent pathway for cholesterol trafficking, resulting in impaired cholesterol efflux and lysosomal accumulation of cholesterol and other lipids. When the NPC1-deficient cells are treated with a high concentration of δ-T, the enhanced lysosomal exocytosis reduces lysosomal accumulation of cholesterol and other lipids, although the defect in the LAL-NPC2-NPC1-dependent pathway is not corrected. However, given the complexity of its mechanism of action, other intracellular pathways may be involved in the vitamin E function that merit further study.

In conclusion, we have demonstrated that δ-T reduces cholesterol accumulation and alleviates cellular phenotypes in NPC1 and Wolman cells. Our data suggest that the pharmacological effect of δ-T may be mediated by stimulating an increase in cytosolic Ca^{2+} that enhances lysosomal exocytosis. This mechanism appears to be independent of either the mutant enzyme or the storage material because we found that δ-T alleviated the lysosomal storage phenotype in other fibroblasts derived from patients with Batten (CLN2), Fabry, Farber, Niemann-Pick disease type A, Sanfilippo type B (MPS IIIB), and Tay-Sachs diseases. Although utilization of δ-T directly as a therapeutic agent is at present limited by its inability to achieve adequate plasma and brain concentrations in both animals and humans, structure optimization to improve its pharmacokinetic properties and increase its plasma and tissue concentrations could lead to the development of a new class of drugs for the treatment of lysosomal storage diseases.

Acknowledgments—We thank Support of Accelerated Research for Niemann-Pick Disease Type C (SOAR-NPC) for fostering a collaborative research environment and stimulating discussion. Mass spectrometry analysis was performed in the Washington University Metabolomics Facility, supported by National Institutes of Health Grant P60 DK020579. We thank Dr. Yiannis A. Ioannou (Mount Sinai School of Medicine) for technical assistance with the exocytosis assays and Ferri Soheilian and Christina Burks for assistance with electron microscopy.

REFERENCES

1. Patterson, M. C., Vanier, M. T., Suzuki, K., Morris, J. A., Carstea, E. D., Neufeld, E. B., Blanchette-Mackie, J. E., and Pentchev, P. G. (2001) Niemann-Pick disease type C. A lipid trafficking disorder. in *The Metabolic and Molecular Bases of Inherited Disease* (Scriver, C. R., Beaudet, A. L., Sly, W. S., and Valle, D., eds) pp. 3611–3633, McGraw-Hill, New York
2. Vanier, M. T., and Millat, G. (2003) Niemann-Pick disease type C. *Clin. Genet.* **64,** 269–281
3. Schulze, H., and Sandhoff, K. (2011) Lysosomal lipid storage diseases. *Cold Spring Harb. Perspect. Biol.* **3,** a004804
4. Wolman, M. (1995) Wolman disease and its treatment. *Clin. Pediatr. (Phila)* **34,** 207–212
5. Ikonen, E. (2008) Cellular cholesterol trafficking and compartmentalization. *Nat. Rev. Mol. Cell Biol.* **9,** 125–138
6. Ory, D. S. (2004) The Niemann-Pick disease genes. Regulators of cellular cholesterol homeostasis. *Trends Cardiovasc. Med.* **14,** 66–72
7. Deffieu, M. S., and Pfeffer, S. R. (2011) Niemann-Pick type C 1 function requires lumenal domain residues that mediate cholesterol-dependent NPC2 binding. *Proc. Natl. Acad. Sci. U.S.A.* **108,** 18932–18936
8. Kwon, H. J., Abi-Mosleh, L., Wang, M. L., Deisenhofer, J., Goldstein, J. L., Brown, M. S., and Infante, R. E. (2009) Structure of N-terminal domain of NPC1 reveals distinct subdomains for binding and transfer of cholesterol. *Cell* **137,** 1213–1224
9. Fielding, C. J., and Fielding, P. E. (1997) Intracellular cholesterol transport. *J. Lipid Res.* **38,** 1503–1521
10. Pérez-Poyato, M. S., and Pineda, M. (2011) New agents and approaches to treatment in Niemann-Pick type C disease. *Curr. Pharm. Biotechnol.* **12,** 897–901
11. Du, H., Cameron, T. L., Garger, S. J., Pogue, G. P., Hamm, L. A., White, E., Hanley, K. M., and Grabowski, G. A. (2008) Wolman disease/cholesteryl ester storage disease. Efficacy of plant-produced human lysosomal acid lipase in mice. *J. Lipid Res.* **49,** 1646–1657
12. Rosenbaum, A. I., Rujoi, M., Huang, A. Y., Du, H., Grabowski, G. A., and Maxfield, F. R. (2009) Chemical screen to reduce sterol accumulation in Niemann-Pick C disease cells identifies novel lysosomal acid lipase inhibitors. *Biochim. Biophys. Acta* **1791,** 1155–1165
13. Davidson, C. D., Ali, N. F., Micsenyi, M. C., Stephney, G., Renault, S., Dobrenis, K., Ory, D. S., Vanier, M. T., and Walkley, S. U. (2009) Chronic cyclodextrin treatment of murine Niemann-Pick C disease ameliorates neuronal cholesterol and glycosphingolipid storage and disease progression. *PLoS One* **4,** e6951
14. Liu, B., Turley, S. D., Burns, D. K., Miller, A. M., Repa, J. J., and Dietschy, J. M. (2009) Reversal of defective lysosomal transport in NPC disease ameliorates liver dysfunction and neurodegeneration in the *npc1*$^{-/-}$ mouse. *Proc. Natl. Acad. Sci. U.S.A.* **106,** 2377–2382
15. Pipalia, N. H., Cosner, C. C., Huang, A., Chatterjee, A., Bourbon, P., Farley, N., Helquist, P., Wiest, O., and Maxfield, F. R. (2011) Histone deacetylase inhibitor treatment dramatically reduces cholesterol accumulation in Niemann-Pick type C1 mutant human fibroblasts. *Proc. Natl. Acad. Sci. U.S.A.* **108,** 5620–5625
16. Chen, F. W., Li, C., and Ioannou, Y. A. (2010) Cyclodextrin induces calcium-dependent lysosomal exocytosis. *PLoS One* **5,** e15054
17. Huang, R., Southall, N., Wang, Y., Yasgar, A., Shinn, P., Jadhav, A., Nguyen, D. T., and Austin, C. P. (2011) The NCGC pharmaceutical collection. A comprehensive resource of clinically approved drugs enabling repurposing and chemical genomics. *Sci. Transl. Med.* **3,** 80ps16
18. Bligh, E. G., and Dyer, W. J. (1959) A rapid method of total lipid extraction and purification. *Can. J. Biochem. Physiol.* **37,** 911–917
19. Han, X., Yang, J., Cheng, H., Ye, H., and Gross, R. W. (2004) Toward fingerprinting cellular lipidomes directly from biological samples by two-dimensional electrospray ionization mass spectrometry. *Anal. Biochem.* **330,** 317–331
20. Lloyd-Evans, E., Morgan, A. J., He, X., Smith, D. A., Elliot-Smith, E., Sillence, D. J., Churchill, G. C., Schuchman, E. H., Galione, A., and Platt, F. M. (2008) Niemann-Pick disease type C1 is a sphingosine storage disease that causes deregulation of lysosomal calcium. *Nat. Med.* **14,** 1247–1255
21. Nagashima, K., Zheng, J., Parmiter, D., and Patri, A. K. (2011) Biological tissue and cell culture specimen preparation for TEM nanoparticle characterization. *Methods Mol. Biol.* **697,** 83–91
22. Sethi, A. A., Stonik, J. A., Thomas, F., Demosky, S. J., Amar, M., Neufeld, E., Brewer, H. B., Davidson, W. S., D'Souza, W., Sviridov, D., and Remaley, A. T. (2008) Asymmetry in the lipid affinity of bihelical amphipathic peptides. A structural determinant for the specificity of ABCA1-dependent cholesterol efflux by peptides. *J. Biol. Chem.* **283,** 32273–32282
23. Norman, A. W., Demel, R. A., de Kruyff, B., and van Deenen, L. L. (1972) Studies on the biological properties of polyene antibiotics. Evidence for the direct interaction of filipin with cholesterol. *J. Biol. Chem.* **247,** 1918–1929
24. Pani, A., Dessì, S., Diaz, G., La Colla, P., Abete, C., Mulas, C., Angius, F., Cannas, M. D., Orru, C. D., Cocco, P. L., Mandas, A., Putzu, P., Laurenzana, A., Cellai, C., Costanza, A. M., Bavazzano, A., Mocali, A., and Paoletti, F. (2009) Altered cholesterol ester cycle in skin fibroblasts from patients with Alzheimer's disease. *J. Alzheimers Dis.* **18,** 829-841
25. Boustany, R. N., Kaye, E., and Alroy, J. (1990) Ultrastructural findings in skin from patients with Niemann-Pick disease, type C. *Pediatr. Neurol.* **6,** 177–183
26. Tietge, U. J., Sun, G., Czarnecki, S., Yu, Q., Lohse, P., Du, H., Grabowski, G. A., Glick, J. M., and Rader, D. J. (2001) Phenotypic correction of lipid storage and growth arrest in Wolman disease fibroblasts by gene transfer of lysosomal acid lipase. *Hum. Gene Ther.* **12,** 279–289
27. Yancey, P. G., Bortnick, A. E., Kellner-Weibel, G., de la Llera-Moya, M., Phillips, M. C., and Rothblat, G. H. (2003) Importance of different pathways of cellular cholesterol efflux. *Arterioscler. Thromb. Vasc. Biol.* **23,** 712–719
28. Schultz, M. L., Tecedor, L., Chang, M., and Davidson, B. L. (2011) Clarifying lysosomal storage diseases. *Trends Neurosci.* **34,** 401–410
29. Klein, D., Büssow, H., Fewou, S. N., and Gieselmann, V. (2005) Exocytosis of storage material in a lysosomal disorder. *Biochem. Biophys. Res. Commun.* **327,** 663–667
30. Medina, D. L., Fraldi, A., Bouche, V., Annunziata, F., Mansueto, G., Spampanato, C., Puri, C., Pignata, A., Martina, J. A., Sardiello, M., Palmieri, M., Polishchuk, R., Puertollano, R., and Ballabio, A. (2011) Transcriptional activation of lysosomal exocytosis promotes cellular clearance. *Dev. Cell* **21,** 421–430
31. Reddy, A., Caler, E. V., and Andrews, N. W. (2001) Plasma membrane repair is mediated by Ca^{2+}-regulated exocytosis of lysosomes. *Cell* **106,** 157–169
32. Qureshi, O. S., Paramasivam, A., Yu, J. C., and Murrell-Lagnado, R. D. (2007) Regulation of P2X4 receptors by lysosomal targeting, glycan protection and exocytosis. *J. Cell Sci.* **120,** 3838–3849
33. Martins, R. M., Alves, R. M., Macedo, S., and Yoshida, N. (2011) Starvation and rapamycin differentially regulate host cell lysosome exocytosis and invasion by *Trypanosoma cruzi* metacyclic forms. *Cell Microbiol.* **13,** 943–954
34. Arantes, R. M., and Andrews, N. W. (2006) A role for synaptotagmin VII-regulated exocytosis of lysosomes in neurite outgrowth from primary sympathetic neurons. *J. Neurosci.* **26,** 4630–4637
35. Gieselmann, V. (1995) Lysosomal storage diseases. *Biochim. Biophys. Acta* **1270,** 103–136
36. Eggermont, E. (2006) Recent advances in vitamin E metabolism and deficiency. *Eur. J. Pediatr.* **165,** 429–434
37. Huang, H. Y., and Appel, L. J. (2003) Supplementation of diets with α-tocopherol reduces serum concentrations of γ- and δ-tocopherol in humans. *J. Nutr.* **133,** 3137–3140
38. Ravaglia, G., Forti, P., Lucicesare, A., Pisacane, N., Rietti, E., Mangialasche, F., Cecchetti, R., Patterson, C., and Mecocci, P. (2008) Plasma tocopherols and risk of cognitive impairment in an elderly Italian cohort. *Am. J. Clin. Nutr.* **87,** 1306–1313
39. Sontag, T. J., and Parker, R. S. (2002) Cytochrome P450 ω-hydroxylase pathway of tocopherol catabolism. Novel mechanism of regulation of vitamin E status. *J. Biol. Chem.* **277,** 25290–25296
40. Sontag, T. J., and Parker, R. S. (2007) Influence of major structural features

of tocopherols and tocotrienols on their ω-oxidation by tocopherol-ω-hydroxylase. *J. Lipid Res.* **48,** 1090–1098
41. Manor, D., and Morley, S. (2007) The α-tocopherol transfer protein. *Vitam. Horm.* **76,** 45–65
42. Bascuñan-Castillo, E. C., Erickson, R. P., Howison, C. M., Hunter, R. J., Heidenreich, R. H., Hicks, C., Trouard, T. P., and Gillies, R. J. (2004) Tamoxifen and vitamin E treatments delay symptoms in the mouse model of Niemann-Pick C. *J. Appl. Genet.* **45,** 461–467
43. Gohil, K., Vasu, V. T., and Cross, C. E. (2010) Dietary α-tocopherol and neuromuscular health. Search for optimal dose and molecular mechanisms continues! *Mol. Nutr. Food Res.* **54,** 693–709
44. Sen, C. K., Khanna, S., and Roy, S. (2006) Tocotrienols. Vitamin E beyond tocopherols. *Life Sci.* **78,** 2088–2098
45. Atkinson, J., Harroun, T., Wassall, S. R., Stillwell, W., and Katsaras, J. (2010) The location and behavior of α-tocopherol in membranes. *Mol. Nutr. Food Res.* **54,** 641–651
46. Royer, M. C., Lemaire-Ewing, S., Desrumaux, C., Monier, S., Pais de Barros, J. P., Athias, A., Néel, D., and Lagrost, L. (2009) 7-Ketocholesterol incorporation into sphingolipid/cholesterol-enriched (lipid raft) domains is impaired by vitamin E. A specific role for α-tocopherol with consequences on cell death. *J. Biol. Chem.* **284,** 15826–15834
47. Hemmerling, J., Nell, S., Kipp, A., Schumann, S., Deubel, S., Haack, M., and Brigelius-Flohé, R. (2010) α-Tocopherol enhances degranulation in RBL-2H3 mast cells. *Mol. Nutr. Food Res.* **54,** 652–660
48. Kruth, H. S., Comly, M. E., Butler, J. D., Vanier, M. T., Fink, J. K., Wenger, D. A., Patel, S., and Pentchev, P. G. (1986) Type C Niemann-Pick disease. Abnormal metabolism of low density lipoprotein in homozygous and heterozygous fibroblasts. *J. Biol. Chem.* **261,** 16769–16774
49. Baxter, L. L., Marugan, J. J., Xiao, J., Incao, A., McKew, J. C., Zheng, W., and Pavan, W. J. (2012) Plasma and tissue concentrations of alpha-tocopherol and delta-tocopherol following high dose dietary supplementation in mice. *Nutrients* **4,** 467–490